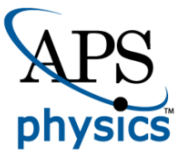



# Channel noise effects on first spike latency of a stochastic Hodgkin-Huxley neuron

Brenton Maisel and Katja Lindenberg

Phys. Rev. E **95**, 022414 — Published 24 February 2017

DOI: 10.1103/PhysRevE.95.022414

# Channel Noise Effects on First Spike Latency of a Stochastic Hodgkin-Huxley Neuron

Brenton Maisel* and Katja Lindenberg
*Department of Chemistry and Biochemistry, and BioCircuits Institute,*
*University of California San Diego, La Jolla, California 92093-0340, USA*

While it is widely accepted that information is encoded in neurons via action potentials or spikes, it is far less understood what specific features of spiking contain encoded information. Experimental evidence has suggested that the timing of the first spike may be an energy-efficient coding mechanism that contains more neural information than subsequent spikes. Therefore, the biophysical features of neurons that underlie response latency are of considerable interest. Here we examine the effects of channel noise on the first spike latency of a Hodgkin-Huxley neuron receiving random input from many other neurons. Because the principal feature of a Hodgkin-Huxley neuron is the stochastic opening and closing of channels, the fluctuations in the number of open channels lead to fluctuations in the membrane voltage and modify the timing of the first spike. Our results show that when a neuron has a larger number of channels, (i) the occurrence of the first spike is delayed and (ii) the variation in the first spike timing is greater. We also show that the mean, median, and interquartile range of first spike latency can be accurately predicted from a simple linear regression by knowing only the number of channels in the neuron and the rate at which presynaptic neurons fire, but the standard deviation (i.e. neuronal jitter) cannot be predicted using only this information. We then compare our results to another commonly used stochastic Hodgkin-Huxley model and show that the more commonly used model overstates the first spike latency but can predict the standard deviation of first spike latencies accurately. We end by suggesting a more suitable definition for the neuronal jitter based upon our simulations and comparison of the two models.

## I. INTRODUCTION

How information is encoded and decoded by neurons is a fundamental question of neuroscience. Although the coding mechanism used by neurons remains unclear, it is widely assumed that coding is based on action potentials or spikes. The most widely assumed coding mechanism is known as rate coding which emphasizes that information that neurons encode about the environment is found in the mean firing rates of neurons [1]. There are three ways to calculate the mean: as the average over the distribution of firing rates over a population of neurons at a fixed time, or as an average of the distribution of firing rates of a single neuron over a long time window, or as an average over a large number of runs of a single neuron [2]. Such coding mechanisms are not without flaws. Averaging over an extended time window is unfeasible: behavioral experiments have shown that a fly can react to stimuli and change flight directions in only 30-40ms [3] and humans can recognize visual scenes in under 150ms [4], so there is simply not enough time for the brain to average over an extended time period. Furthermore, it is easier experimentally to record a single neuron and average over $N$ runs than it is to record $N$ neurons in a single run, so experimental evidence rests on the assumption that there are populations of neurons with similar properties. Based on these issues of timing and the requirement that neurons in a population be essentially identical, the idea of "rate coding" by all of these methods has been routinely criticized [5–7].

An alternative coding mechanism, known as first spike latency coding, has been used as a meaningful strategy to understand information encoding by neurons. First spike latency is defined as the time of the first spike relative to stimulus onset. In [4], Thorpe argues that the brain does not have time to evaluate more than one spike from each neuron for each step of processing behavioral responses to a stimulus. Therefore, the first spike should contain most of the relevant information, and several groups have shown that most of the information about a new stimulus is conveyed very quickly [8–11]. In 2004, the first direct evidence showing first-spike coding in humans was released [12]. In this experiment, Johansson et al. applied objects of various shapes to fingertips at various angles and forces. They showed that the first spikes contained reliable information about the direction of fingertip force and object shape. Moreover, it provided information faster than rate coding did. While we do not claim that either rate coding or first spike latency coding is the correct one (and recent publications suggest that both methods are used for information encoding in animals [13–16]), we focus on first spike latency as an informative mathematical problem and potential coding mechanism.

In this study, we investigate the first spike latency of a Hodgkin-Huxley neuron. We select this neuron for study because of its close connection to biological reality and its ability to reproduce almost all single-neuron propeties [17–19]. One defining property of the Hodgkin-Huxley neuron model that allows for action potential generation is the existence of sodium and potassium channels which transition between open and closed states with voltage-dependent rate constants. Each channel is composed of four gates: the sodium channel is composed of three ac-

*Electronic address: bmaisel@ucsd.edu

tivating gates (known as type m gates) and one inactivating gate (known as a type h gate), and the potassium channel is composed of four activating gates of type n. At rest, the activating gates are closed and the inactivation gate is open, but as a neuron receives synaptic input from other neurons, the membrane voltage rises, causing the activating gates to open, which starts the depolarization of the membrane potential. When the voltage is high enough, the sodium inactivation gate closes while the potassium gates remain open, which repolarizes the membrane potential. The dynamics of the $n$ gates and $m$ gates are similar, but the $n$ gate dynamics are on a slower time scale [20].

A channel can only conduct when it is considered open, and a channel is considered open when all the gates within the channel are open. The most direct approach to modeling the open and closing of channels is referred to as the Markov Chain model. In the Markov Chain model, each of $N$ channels of a particular type functions as a Markov process, where the channel transitions independently among discrete configurations, creating a continuous-time Markov Chain with voltage-dependent transition rates. However, simulating such a Markov Chain is computationally exhaustive, so we use a set of stochastic differential equations developed by Fox and Lu which well approximates the behavior of the Markov Chain model [21]. The stochastic equations of Fox and Lu do not modify the determinstic structure of the Hodgkin-Huxley equations, and they include stochastic perturbations which account for the opening and closing of channels. We refer to these stochastic perturbations as channel noise to be consistent with previous literature [22, 23]. This model was numerically simulated and agrees remarkably well with dynamical behavior predicted by the Markov Chain model of the channel states [22, 23]. Our goal is to understand how channel noise affects the timing of first spike latency.

Neurons in networks receive input from other neurons within the network. Experimental studies have shown that synapses transmit signals in an unreliable fashion due to stochastic release of transmitters, and so not every presynaptic spike elicits a postsynaptic response [24–26]. Experimental evidence shows that only $10-30$ percent of presynaptic spikes may elicit any postsynaptic response [27, 28]. To the best of our knowledge, the first spike time of a Hodgkin-Huxley model with channel noise and stochastic input from presynaptic neurons has not been simulated and is the focus of this paper.

Our paper is organized as follows: In Sec. II we give a mathematical description of the stochastic Hodgkin-Huxley neuron with unreliable synaptic input as well as discuss how we analyze first spike latency from a statistical perspective. Then in Sec. III we analyze how the parameters of the model affect these first spike latency times and the distribution of the times. In addition, we study what effect the number of channels in a Hodgkin-Huxley neuron has on the first spike latency. We then conclude with some closing remarks in Sec. IV.

## II. THE MODEL

The deterministic dynamics of the Hodgkin-Huxley model [17] are given by the following set of differential equations

$$\begin{aligned} C\dot{V} &= I_{syn}(t) - \bar{g}_{Na}m^3h(V-E_{Na}) \\ &- \bar{g}_K n^4(V-E_K) - \bar{g}_L(V-E_L) \\ \dot{n} &= \alpha_n(V)(1-n) - \beta_n(V)n \\ \dot{m} &= \alpha_m(V)(1-m) - \beta_m(V)m \\ \dot{h} &= \alpha_h(V)(1-h) - \beta_h(V)h, \end{aligned} \tag{1}$$

where

$$\begin{aligned} \alpha_n(V) &= \frac{0.01(V+10)}{\exp[(V+10)/10]-1} \\ \beta_n(V) &= 0.125\exp[V/80] \\ \alpha_m(V) &= \frac{0.1(V+25)}{\exp[(V+25)/10]-1} \\ \beta_m(V) &= 4\exp[V/18] \\ \alpha_h(V) &= 0.07\exp[V/20] \\ \beta_h(V) &= \frac{1}{\exp[(V+30)/10]+1}. \end{aligned}$$

The values of the parameters along with definitions are found in Table I. The parameters have been chosen to match biological values [17] and shifted so that the equilibrium membrane potential of our Hodgkin-Huxley neuron is set to 0 mV.

TABLE I: Parameter values used for simulation of the Hodgkin-Huxley model. The resting potential has been set to 0 mV

| Parameter | Definition | Value |
|---|---|---|
| $C$ | membrane capacitance | $1\mu F/cm^2$ |
| $E_{Na}$ | sodium reversal potential | $120mS/cm^2$ |
| $E_K$ | potassium reversal potential | $36mS/cm^2$ |
| $E_L$ | leak reversal potential | $0.3mS/cm^2$ |
| $\bar{g}_{Na}$ | maximal sodium conductance | $115mV$ |
| $\bar{g}_K$ | maximal potassium conductance | $-12mV$ |
| $\bar{g}_L$ | maximal leak conductance | $10.6mV$ |

The channel conductances $\bar{g}_K$ and $\bar{g}_{Na}$ are the produts of two factors: an individual channel conductance on the order of picosiemens and the number of channels in the area $A$ (given by $N_{Na}$ for the number of sodium channels and $N_K$ for the number of potassium channels). The sodium channel density is therefore the value $N_{Na}/A$ and likewise $N_K/A$ for potassium channel density which we will use when discussing the stochastic model. Not every channel is open at the same time, and so the equations account for this by multiplying the conductances by a factor describing the fraction of channels open at a given time. For sodium channels, this factor is given by the

$m^3h$ term since each sodium channel has three activation gates of type $m$ and one inactivation gate of type $h$. Similarly, the $n^4$ term is used for potassium channels as each potassium channel consists of four independent activation gates of type $n$ [17, 21]. For this paper, we assume that the sodium channel density is given by $60\mu m^{-2}$ and the potassium channel density by $18\mu m^{-2}$, where the ratio is derived from biophysical neuron parameters [22, 29].

Generally, a presynaptic neuron connects to over $10^4$ postsynaptic neurons, and estimates are that the brain is composed of 100 billion neurons, so each neuron connects to many others and is connected to many others [2]. To simplify matters, we assume that our Hodgkin-Huxley neuron receives current from presynaptic neurons which spike at some rate $\lambda$. We let $\lambda$ be the same for each presynaptic neuron. We express such a presynaptic current as follows:

$$\begin{aligned} I_{syn}(t) &= Q\left[\sum_{k=1}^{N_e}\sum_{l} h_k^l \delta(t-t_k^l)\right. \\ &\quad \left. - \sum_{m=1}^{N_i}\sum_{n} h_m^n \delta(t-t_m^n)\right]. \end{aligned} \tag{2}$$

In this equation, $N_e$ is the number of excitatory presynaptic neurons, $N_i$ the number of inhibitory presynaptic neurons, $Q = C\Delta V$ represents the charge associated with each voltage change $\Delta V$, $t_k^l$ is the discharge time of the $l^{th}$ spike at the $k^{th}$ excitatory presynaptic neuron, and similar notation represents the inhibitory presynaptic neurons [30]. To account for the fact that not every presynaptic spike elicits a postsynaptic response [24–26], we introduce the random variable $h_k^l$ where $h_k^l = 1$ with probability $p$ (the probability of a successful postynaptic response) and $h_k^l = 0$ with probability $1-p$ (the probability of no postsynaptic response). As we indicated earlier, experimental evidence suggests that reasonable values for the parameter $p$ are in the range $0.1 - 0.3$ [27, 28].

First we choose the values for the parameters in the $I_{syn}(t)$ expression [Eq. (2)]. Each excitatory presynaptic neuron which induces a voltage change to our Hodgkin-Huxley model instantaneously increases the voltage by a value of $Q$ which for this model will be set to $0.5mV$. This value is near experimental observations for neurons in the rat visual cortex and the cat visual cortex [31–35]. Experiments have shown that mammalian vestibular nucleus neurons fire spontaneously in the awake animal at baseline firing rates of $30 - 100$ Hz (and can increase to several hundred Hz) [36, 37] (in humans 40 Hz is considered a typical firing rate associated with consciousness) [38]. Thus in order to see the trend of first firing times as a function of the spiking rate of presynaptic neurons, we focus on the interval of $30 - 100$ Hz. We further assume that the number of presynaptic neurons is 2000 (since only a fraction of the $10^4$ presynaptic neurons will provide input) and the excitatory to inhibitory ratio of the presynaptic neurons is $N_e : N_i = 4 : 1$, the ratio found in the mammalian cortex [39]. While we do not claim that these parameter values are exact across all species, they are biologically plausible values which allow us to examine how the first spike latency time is affected by underlying parameters in the model.

In the limit of infinitely many channels, $m^3h$ and $n^4$ accurately model the fraction of open channels. Real neurons, on the other hand, only have finitely many channels, so fluctuations in the number of open channels have an effect on the membrane voltage. The channel noise model developed by Fox and Lu is a stochastic version of the Hodgkin-Huxley system to include fluctuations in the number of open channels. The Fox and Lu system to account for finitely many channels is given by the following twelve stochastic differential equations [21, 22]:

$$\begin{aligned} C\dot{V} &= [I_{syn}(t) - \bar{g}_{Na} y_{31}(V - E_{Na}) - \bar{g}_K x_4 (V - E_K) - \bar{g}_L (V - E_L)] \\ \dot{\mathbf{x}} &= A_K \mathbf{x} + 4\alpha_n x_0 \mathbf{e_1} + \frac{1}{\sqrt{N_K}} S_K \xi_K \\ \dot{\mathbf{y}} &= A_{Na}\mathbf{y} + 3\alpha_m y_{00}\mathbf{e_1} + \alpha_h y_{00}\mathbf{e_4} + \frac{1}{\sqrt{N_{Na}}} S_{Na}\xi_{Na}. \end{aligned} \tag{3}$$

The vector $\mathbf{x}$ is composed of components $x_i$, $(i = 1, 2, 3, 4)$, representing the proportion of potassium channels with $i$ open gates of type $n$. The entries of $\mathbf{y}$ are denoted as $y_{ij}$, $(i = 0, 1, 2, 3$ and $j = 0, 1)$, representing the proportion of sodium channels with $i$ open $m$ subunits and $j$ open subunits of type $h$. The quantities $x_0$ and $y_{00}$ are defined by using the fact that $\sum_i x_i = 1$ and similarly for the $y$ vector. The vectors $\mathbf{e_i}$ are unit vectors with 1 in the $i^{th}$ entry. The matrices $A_K$, $A_{Na}$, $S_K$, and $S_{Na}$ are given in the appendix. Moreover, $\xi_K$ and $\xi_{Na}$ are vectors of independent Gaussian white noise terms. While the system above is valid for a large number of channels, it has been shown to be a very accurate representation of the Markov chain model even for a small number of channels [22].

We are interested in understanding the time to first

spike and the variability of this spiking time across trials. A spike occurs when the voltage $V(t)$ crosses some threshold $\theta$. Hence we define the random variable $T$ as

$$T = \inf\{t \geq 0 | V(t) \geq \theta\}. \quad (4)$$

We consider $\theta$ to be a fixed constant of approximately $35mV$, although the exact value is not important since it shifts the spike time by only a fraction of a milisecond. In order to study typical first firing times, many studies have looked at the expectation of $T$, denoted by $\langle T \rangle$, and the trial-to-trial variability (or jitter) of $T$ defined as the standard deviation of $T$. These values generally provide useful information when the distribution is not skewed. However, based on our simulations of Eq. (3), the distribution of spike times is heavily skewed (see Fig. 1). For this reason, we choose instead to compare median values as a better measure of the central tendency of data and to use the interquartile range (IQR) as a better measure of trial-to-trial variability, where the interquartile range is defined to be the difference between the first quartile and third quartile of a data set. Median first spike latencies and IQRs have begun to be used more in biological experiments [40, 41], but actual simulations comparing these values to those of means and standard deviations have, to the best of our knowledge, not been done.

The parameters of Eq. (3) that we vary in these simulations are the presynaptic firing rates, the probability of successful transmission of presynaptic spikes to our Hodgkin-Huxley neuron, and the number of channels in the neuron. As the number of channels grows, the dynamics of the stochastic Hodgkin-Huxley neuron converges to that of the deterministic Hodgkin-Huxley model. From the structure of the stochastic Hodgkin-Huxley model [Eq. (3)], it is clear that fewer channels lead to stronger fluctuations. Furthermore, having $N_e$ independent excitatory presynaptic neurons, each firing at rate $\lambda$, is statistically equivalent to having one excitatory presynaptic neuron firing at rate $\lambda N_e$. To account for the less than certain successful transmission from the presynaptic neuron, we modify this rate term to be $\lambda N_e p$, where $p$ is the probability of a successful transmission. Since $N_e$ is a fixed parameter, we can eliminate one parameter by considering $\lambda p$ as a single parameter and thus viewing the probability term $p$ as rescaling the rate. Thus, the two parameters we will look at are the product $\lambda p$ which we will refer to as the "effective rate" and the number of channels ($N_K$ and $N_{Na}$). The parameters we use for the numbers of channels can be found in Table II.

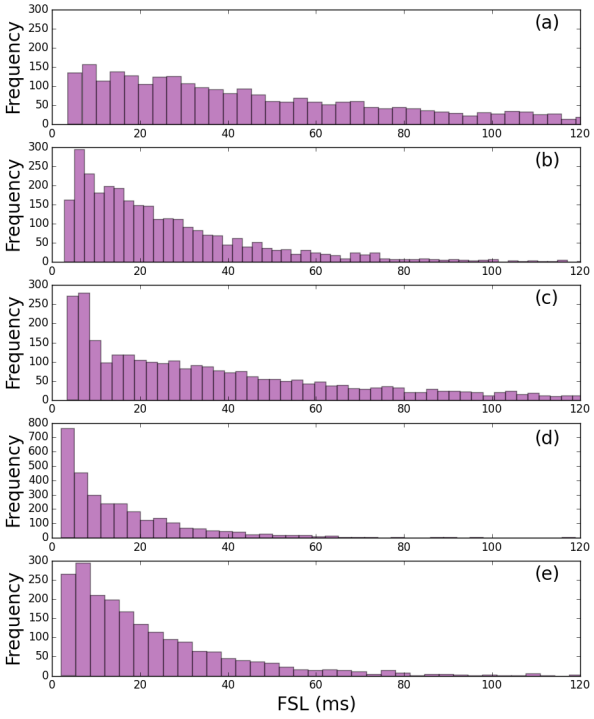


FIG. 1: (Color online) Examples of the distribution of first spiking times obtained from the set of equations Eq. (3) showing positive skewness. Parameters used for low noise plots (panels (a) and (c)) were $N_{Na} = 1800$, and $N_K = 540$ while for high noise plots (panels (b) and (d)), they were $N_{Na} = 600$, and $N_K = 180$. For low rate plots (panels (a) and (b)), the parameters for the synaptic input current were $\lambda = 25$ Hz and $p = 0.10$, while for high rate plots (panels (c) and (d)), the parameters were $\lambda = 100$ Hz and $p = 0.30$. Panel (e) shows no channel noise with high synaptic input.

TABLE II: Membrane area and corresponding number of channels

| Membrane Area | Number of Channels | |
|---|---|---|
| $(\mu m^2)$ | $N_{Na}$ | $N_K$ |
| 5 | 300 | 90 |
| 10 | 600 | 180 |
| 20 | 1200 | 360 |
| 30 | 1800 | 540 |

## III. RESULTS AND DISCUSSION

All simulations were based on the system of stochastic differential equations Eq. (3). We used the Euler-Maruyama method [42, 43] with time step $\Delta t = 50\mu s$ and with 2000 presynaptic neurons providing spike train inputs of rate $\lambda$. Initial conditions were given by the resting state of the neuron shifted so that $V(0) = 0$ mV. The mean first spike latency is defined as $\langle t \rangle = \frac{1}{N}\sum_{i=1}^{N} t_i$ where $N$ is the number of trials (we used $N = 1000$) and $t_i$ is the time of the first spike for the $i^{th}$ trial. The standard deviation (or jitter) is defined as $J = \sqrt{\langle t^2 \rangle - \langle t \rangle^2}$ [30, 44, 45]. The median is defined as $t_{(\frac{N}{2})}$ and the in-

terquartile range is defined as $t_{(\frac{3N}{4})} - t_{(\frac{N}{4})}$ where $t_{(j)}$ is the $j^{th}$ order statistic.

We first discuss the behavior seen in Fig. 1. The histograms shown in Fig. 1 are based on 2,000 simulations of Eq. (3). The input current into the Hodgkin-Huxley neuron determines its firing rate. Ignoring the stochasticity of the input current for the moment, the neuron is in the silent regime (i.e. no firing) for $I < 6.27\mu A/cm^2$, in a bistable regime where the fixed point coexists with a stable limit cycle for $6.27\mu A/cm^2 < I < 9.78\mu A/cm^2$, and in a periodic firing regime for $I > 9.78\mu A/cm^2$. Taking the stochasticity into account, the average stimulating current $\bar{I}_{syn}$ determines the dynamical regime of the neuron. Following Luccioli et al. [46], the average stimulating current is given by $\bar{I}_{syn} = C\lambda p\Delta V(N_e - N_i)$. With the parameters defined earlier, this simplifies to $\bar{I}_{syn} = (0.6\mu A \cdot s/cm^2)\lambda p$. Therefore, the low input current panels in Fig. 1 [panels (a) and (b)] presents a stochastic neuron in the silent regime, and the high input current [panels (c) and (d)] illustrate a stochastic neuron in the periodic firing regime.

In our model, there are two mechanisms that lead a neuron to fire: the stochastic synaptic current and the intrinsic channel noise. Therefore, we expect to see some juxtaposition of the distributions from both sources in the first spike latency distributions in Fig. 1 [46, 47]. The multipeak distributions in panel (b) (low firing rate panel) shows this clearly: each peak is primarily due to one or the other of the two firing mechanisms. Further evidence of the reasoning behind the multipeaks can be observed in panel (e) in which the channel noise has been eliminated. With the absence of this extra source of noise, the histogram lacks a multipeaked distribution. The very small fluctuations in the channel noise lead to a distribution with a very long tail as seen in panel (a). This tail overlaps with and masks the low synaptic input peak. This behavior is similar to that illustrated by Luccioli et al. for the low rate behavior [46]. Increases in the average synaptic current and in the amplitude of intrinsic channel noise lead to faster first spike latency, which is consistent with the fact that a neuron fires as soon as a threshold value is reached. The associated shift in the distribution toward a faster first spike latency and less heavy tails is seen in panels (c) and (d) of Fig. 1. As both of these current increases lead to a shortening of the first spike latency, the multipeaks tend to merge at the low end and the resulting distributions are smoother than in the low firing rate cases illustrated in panels (a) and (b). As we will see in the next sections, some statistical properties of these distributions can be accurately modeled by a linear regression depending on the synaptic input rate and the intrinsic channel noise.

Our next goal is to compare the mean with the median and the IQR with the standard deviation of the distribution of first spike latencies for different channel areas and effective rates (recall that the effective rate is the quantity $\lambda p$, where $\lambda$ is the Poisson rate of each presynaptic neuron and $p$ is the probability of successfully producing a postsynaptic response).

### A. Mean/Standard Deviation vs. Median/IQR

As previously stated, the skewness of the data suggests using the median and IQR to analyze typical first spike latencies and the IQR to study their variability rather than using the mean and standard deviation. For each of the channel areas in Table II, we plotted the resulting values of means, medians, IQRs, and standard deviations, see Fig. 2. We then calculated the Pearson Correlation Coefficients $r$ [48] to measure the strength of correlation between the statistics of interest and the effective firing rate, the results of which are shown in Table III .

TABLE III: Pearson Correlation Coefficients $r$ of the relationship between Effective Rate and Statistical Measures for various Membrane Areas

| Membrane Area | Mean | Median | IQR | Standard Deviation |
|---|---|---|---|---|
| 5 | -.9376 | -.9690 | -.9070 | -.6959 |
| 10 | -.9783 | -.9764 | -.9362 | -.6955 |
| 20 | -.9583 | -.9757 | -.9515 | -.6061 |
| 30 | -.9659 | -.9710 | -.9529 | -.7335 |

Since neuronal first spike latency (FSL) is heavily determined by firing rates of input neurons [49], we would like to be able to predict the median firing time knowing the effective rate. For this reason, the Pearson's Correlation Coefficient gives us an idea about how linear the data is, and thus values close to $r = -1$ suggest we can closely estimate the statistics of the first spike latency. We first note that the mean and median values are both strongly correlated with the effective rate, with the median first spike time slightly more correlated with the effective rate. The values of the mean first spike latency are greater than those of the median first spike latency, which results from the positive skewness of the data. One naturally expects that when there is an increase in input from the presynaptic neurons, the postsynaptic neuron should fire sooner. In fact, that trend is observed in Fig. 2, where we show data from simulations when the membrane area is $10\mu m^2$ and $30\mu m^2$ as a representative sample of statistical behavior. We can therefore see that the effective rate can be used as a good predictor for determining the values of the mean and median first spike latencies. This is a key result of this work: despite the randomness of the presynaptic input and the randomness of the intrinsic channel noise, a simple linear regression yields high accuracy for predicting a number of statistical properties of the distribution of first spike latencies for a biologically plausible range of values.

The results in Table III suggest that IQR is a better measure for the spread of the first spike latencies than

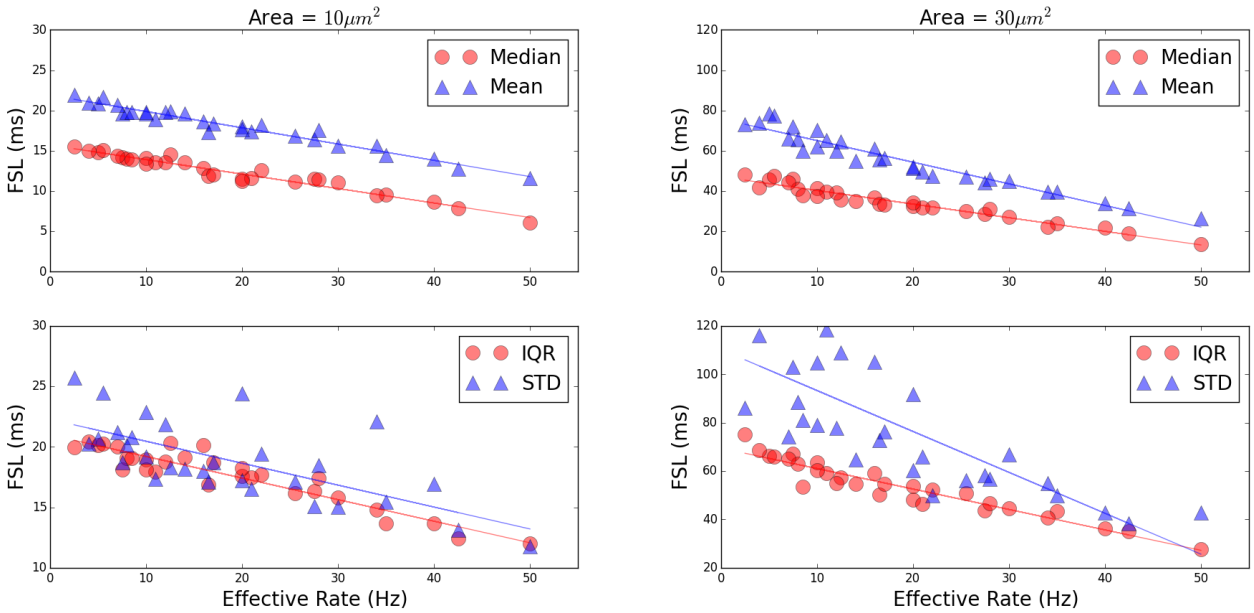


FIG. 2: (Color online) Plots of the mean, median, IQR, and standard deviation (STD) of the result of 1000 simulations of the set of equations Eq. (3) for each value of effective rate for two channel areas ($10\mu m^2$ and $30\mu m^2$). The plots show that the mean, median, and IQR are modeled exceptionally well by a linear function, whereas the standard deviation is not.

the standard deviation, and that the effective rate more accurately predicts the spread of data in terms of IQR compared to the standard deviation. The reason is that the combination of the stochastic opening and closing of channels along with unreliable synaptic input can cause large outliers due to noise being able to drive voltage away from the threshold thereby delaying the time to first spike. These outliers have a much stronger effect on the standard deviation than on the IQR. For this reason, the effective rate does a poorer job estimating the neuronal jitter than it does estimating the IQR as a measure of the spread of the data. We also see that for a fixed channel area, there is much more variability in the measurements of standard deviation for smaller effective rates, but that the spread decreases as the effective rate increases. This is due to the fact that when the effective rate is higher, the postsynaptic neuron receives more input and therefore the voltage drifts toward the threshold more quickly, thereby reducing the probability of an outlier.

### B. Effect of Channel Number on FSL

We now explore the effect of changing the number of channels on the distribution of first spike latencies. As a result of Eq. (3), increasing the number of channels reduces the fluctuations in voltage due to the stochastic opening and closing of the gates. Figure 3 shows the median first spike latency as the channel area increases for various values of the effective rate. For clarity, we do not include every effective rate value used in the previous section, but we use a sufficiently broad range in order to understand trends in the behavior of first spike latency times.

We recall that the number of sodium channels is $60 \times A$ where $A$ is the channel area (in units of $\mu m^2$), and the number of potassium channels is $18 \times A$. That is, the total number of channels is directly proportional to the channel area. From the structure of Eq. (3), we know that the Wiener processes are scaled by a factor of $N^{-1/2}$, where $N$ is the number of channels. By increasing the channel area, the variance of the Wiener processes decreases by a factor proportional to $N^{-1} \propto A^{-1}$, and so a larger number of channels of a neuron leads to a smaller effect of the stochastic opening and closing of the gates within the channels.

We first discuss the effect of channel noise on the median first spike latency. From Fig. 3, we see that as the number of channels increases, there is a delay in the median time to spike as well as an increase in the spread of firing times. Conversely, when there are fewer channels, the median times until first firing are close to each other regardless of synaptic input rate. Because there are more excitatory than inhibitory neurons, the presynaptic neurons provide a net positive voltage increase, so there is a net drift for the voltage to increase toward the firing threshold. The simulations show that the presence of noise helps to accelerate this voltage increase. Addition-

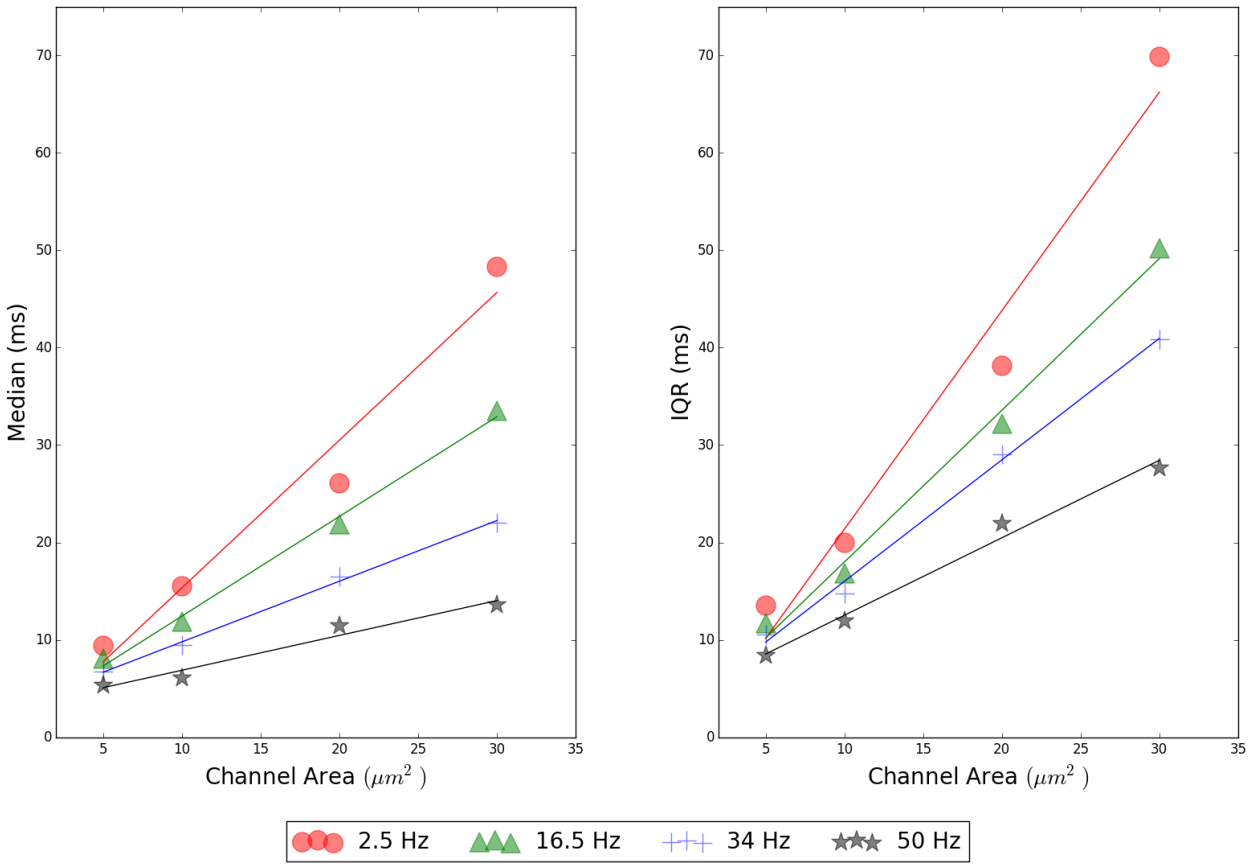


FIG. 3: (Color online) Median first spike latency and IQR for various effective firing rates as a function of the change in the number of channels in the Hodgkin-Huxley neuron. Lines show best fit linear regression for various effective rates. Top line to bottom line show best linear fits for circles, triangles, pluses, and stars respectively.

ally, we note that when the noise is weaker (i.e., when there is a larger number of channels), the median firing time can nevertheless be short for strong enough synaptic input. Because there are two sources of stochastic effects, the channel noise and the synaptic input fluctuations, it follows that when the channel noise in the neuron is weak, the synaptic input becomes the primary factor for voltage fluctuations. This effect is observed in Fig. 3.

As discussed in the previous section, we find the IQR to be a better measure of the spread of first spike latency statistics than the standard deviation. For this reason, we show the IQR instead of the standard deviation in Fig. 3. The effects observed for the IQR are essentially the same as those observed for the median.

### C. Comparison to Subunit Noise Model

An alternative model to incorporate stochasticity into each gating variable is referred to as the subunit noise model, where each gating variable equation in the original Hodgkin-Huxley model is perturbed by Gaussian white noise. This set of stochastic differential equations was first proposed by Fox and Lu as a Langevin equation description for the dynamics of the subunits, and was derived by applying a system size expansion to the states of populations of subunits [21]. Such a system is represented by the following set of stochastic differential equations:

$$\begin{aligned} C\dot{V} &= I_{syn}(t) - \bar{g}_{Na} m^3 h (V - E_{Na}) \\ &\quad - \bar{g}_K n^4 (V - E_K) - \bar{g}_L (V - E_L) \\ \frac{dn}{dt} &= \alpha_n(V)(1-n) - \beta_n(V) n + \xi_n(t) \qquad (5) \\ \frac{dm}{dt} &= \alpha_m(V)(1-m) - \beta_m(V) m + \xi_m(t) \\ \frac{dh}{dt} &= \alpha_h(V)(1-h) - \beta_h(V) h + \xi_h(t) \end{aligned}$$

(6)

where the $\xi$'s are independent Gaussian white noises with zero mean and covariance function

$$\langle \xi_x(s)\xi_x(t)\rangle = \frac{\alpha_x(1-x)+\beta_x x}{N}\delta(t-s).$$

Here, $x$ is either $m, h$, or $n$, and $N$ is the number of $Na^+$ channels for the $m$ and $h$ subunits or the number of $K^+$ channels for the $n$ subunits. Equations (5) have been used extensively to account for fluctuations in the gating variables and hence in the fraction of open channels [50–54]. One reason for its popularity is that it maintains the original structure of the Hodgkin-Huxley model (with the addition of noise terms). Despite its widespread use, numerical studies have revealed inaccuracies such as voltage fluctuations that are too weak [55], firing rates that are too low (and hence mean interspike intervals that are too long), and overstated information transfer rates [56]. Such discrepancies can be explained as follows: the quantities $m$, $h$, and $n$ represent the fraction of open subunits, whereas the quantities that influence the membrane potential are the products $m^3h$ and $n^4$, the fraction of open channels. In the limit of infinitely many channels, $m^3h$ and $n^4$ correctly model the fraction of open channels, but for finitely many channels, there is no guarantee that fluctuations in these terms will model fluctuations in the total fraction of open channels. In other words, the subunit noise model assumes that $\langle m^3h\rangle = \langle m\rangle^3\langle h\rangle$, which is not correct for a neuron with only finitely many channels.

Let us consider a case study of the subunit noise model Eq. (5) using an area of $30\mu m^2$. The plots of the median, mean, standard deviation, and IQR are shown in Fig. 4. The Pearson correlation coefficients are: mean (-.9781), median (-.9694), standard deviation (-.9714), and IQR (-.9528). The standard deviation for the subunit noise model has a much stronger linear correlation with the effective rate $\lambda p$ of presynaptic neuron firing than the channel noise model. As discussed in [55], the fluctuations in membrane voltage due to the intrinsic noise are much weaker than those resulting from the synaptic input from presynaptic neuron. Because the inputs from the presynaptic neurons cause the membrane voltage to have a net drift toward the threshold, the probability of having a first spike time which deviates greatly from the mean spiking time is very small. Therefore, we expect the values for the mean, median, IQR, and standard deviation to have strong correlation values, which is observed in Fig. 4.

Moreover, for a membrane area $A = 30\mu m^2$, the subunit noise model typically has a larger mean, median, and IQR but a smaller standard deviation than the channel noise model (with the value of the IQR larger than that of the standard deviation). As pointed out in [56], the subunit noise model has a longer mean spike interval (i.e. lower firing rate). For that reason, we expect an overall delay in the time until the first spike and hence we see an increase in the mean and median first spike latency, and this delay is observed in our simulations. We also

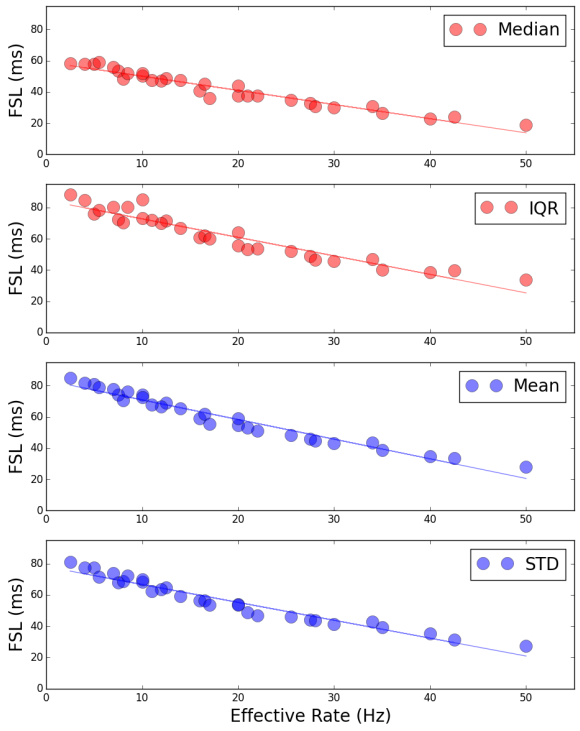


FIG. 4: (Color online) Plots of the subunit noise model Eq. (5) comparing the median (top plot), IQR (second plot), Mean (third plot), and the standard deviation (bottom plot) for different values of the effective rates $\lambda p$ for the case when noise perturbs subunit fractions. The parameter for the area of the neuron is $A = 30\mu m^2$.

observed that although some trials had a large first spike latency, they did not deviate as far from the central tendency of the distribution as they did in the channel noise model. The delay in the mean and median first spike latency as well as the observation of large first spike latency times which are relatively closer to the median of the distribution compared to the channel noise model explains the increase in IQR and the lower value for standard deviation in the former.

Although the subunit noise model maintains the original structure of the Hodgkin-Huxley neuron model, the subunit noise model and the channel noise model show widely different behavior for the standard deviation of first spike latencies for different effective rates and channel areas. As previous literature has shown [55, 56], the channel noise model maintains high accuracy for predicting the original Markov Chain model whereas the subunit model does not. Our numerical results imply that the traditional definition of neuronal jitter (standard deviation) is not an appropriate statistical measure of first spike latency. The fact that standard deviation is well-predicted in the inaccurate subunit noise model

and poorly predicted in the more accurate Fox and Lu model [Eq. (3)] suggests that the traditional definition of neuronal jitter is ill-suited for describing variations in the first spike latency.

## IV. CONCLUSIONS

In this paper, we have sought to examine the effects of channel noise on first spike latency. Because real neurons have finitely many channels, the stochastic opening and closing of these channels leads to fluctuations in the membrane voltage that are not accounted for in the deterministic Hodgkin-Huxley model. In order to account for these fluctuations, we used the Fox and Lu system size expansion model because (a) it is a highly accurate approximation to the gold standard Markov Chain, and (b) it is a far more computationally efficient model than the Markov Chain [21, 22]. We first looked at statistical descriptions of the first spike latency, and we demonstrated that the median/IQR were better statistical descriptions of the first spike latency distribution than the mean/standard deviation. We noted that the distribution of spike times is positively skewed, which leads to poor predictions of the neuronal jitter (defined as the standard deviation of the spike latency distribution). Moreover, we established the surprising result that statistics of the first spike latency distribution could be accurately predicted by a simple linear regression despite the presence of both intrinsic channel noise and the randomness of synaptic input from other neurons in the network. Our work suggests that despite the randomness within the model, accurate measures of parameters of a stochastic neural system can lead to highly accurate predictions of first spike latencies through a simple linear function.

We then analyzed the effect of channel noise on the median first spike latency and on the IQR of first spike latencies. We showed that as the channel number increases, the effective firing rate becomes the determining factor in the distribution of first spike latencies. This is due to the fact that increasing the channel number decreases the amplitude of the fluctuations in the membrane voltage, so the residual fluctuations in voltage are increasingly due to the randomness of presynaptic neural firing. The results from our simulations agree with previous literature that channel noise contributes importantly to spike timing by increasing fluctuations in spike timing but decreasing first spike latency [57]. An application of such a result is in "stochastic facilitation," or the improvement of information processing due to noise. As we previously noted, we showed that the presence of channel noise in a neuron causes spiking to occur more quickly. Bi and Poo showed that when the postsynaptic neuron fires within $20ms$ after the presynaptic neuron fires, the synaptic efficacy increases, leading to long-term potentiation [58]. Our results would suggest that the fluctuations of the membrane potential due to the stochastic opening and closing of membrane channels helps facilitate spike-timing dependent plasticity.

Lastly, we showed that the standard deviation may be an inappropriate definition for studying first spike latency variations. To understand why, we compared the channel noise model to that of a subunit noise model in which the individual gating variables themselves are perturbed with independent Gaussian white noise. The subunit noise model was first introduced by Fox and Lu as a simplification of their system size expansion [21]. The subunit noise model is more commonly used due to the fact that it retains the original structure of the Hodgkin-Huxley model. As we noted earlier, the subunit noise model assumes that $\langle m^3 h \rangle = \langle m \rangle^3 \langle h \rangle$, which is generally not true when the system contains finitely many channels. This assumption leads to weaker voltage fluctuations and lower firing rates [55, 56]. Our simulations show that compared to the channel noise model, the subunit noise model increases the mean and median time to first spike but decreases the neuronal jitter. The neuronal jitter can be predicted far more accurately from knowing the effective rate in the subunit noise model than in the channel noise model. In other words, using standard deviation as a definition for neuronal jitter is accurate only for the subunit noise model and not for the channel noise model. However, this may lead to serious errors in model applications because the channel noise model is much more accurate (closer in replicatng dynamics of the Markov Chain model) than the subunit noise model for describing neurons with biological channel noise. For this reason, we suggest that the IQR rather than the standard deviation is a more appropriate measure of the spread of first spike latencies.

To summarize, the main contributions of our paper are (a) to demonstrate that the median and IQR are better statistical measures to describe the first spike latency distribution than the mean/standard deviation, (b) to demonstrate that a simple linear regression is highly accurate for estimating the IQR, mean, and median first spike latency from knowing only the effective firing rate for different numbers of channels, and (c) to provide evidence that using standard deviation as a measure of neuronal jitter may be improperly applied as a result of using the more common subunit noise model despite its inaccuracy by producing weaker voltage fluctuations than predicted by the Markov Chain model.

As a continuation of this work, we are in the process of studying the effects of channel noise on the synchronization of neurons in a network. Research has shown a strong correlation between abnormal synchronization and brain disorders including epilepsy, Parkinson's disease, Alzheimer's disease, and schizophrenia. Studying the effects of channel noise on synchronization provides a mathematical framework towards understanding how neurons regulate synchronization in the presence of noise [59–61].

**Acknowledgments**

We wish to acknowledge Sadique Sheik for his assistance in developing numerical simulations. We gratefully acknowledge support by the U. S. Office of Naval Research (ONR) under Grant No. N00014-13-1-0205.

**Appendix**

The matrices used for numerical simulations and included in Eq. (3) are defined as:

$$A_K = \begin{bmatrix} -3(\alpha_n+\beta_n) & 2\beta_n & 0 & 0 \\ 3\alpha_n & -2(\alpha_n+\beta_n) & 3\beta_n & 0 \\ 0 & 2\alpha_n & -(\alpha_n+3\beta_n) & 4\beta_n \\ 0 & 0 & \alpha_n & -4\beta_n \end{bmatrix}$$

$$A_{Na} = \begin{bmatrix} -(2\alpha_m+\beta_m+\alpha_h) & 2\beta_m & 0 & 0 & \beta_h & 0 & 0 \\ 2\alpha_m & -(\alpha_m+2\beta_m+\alpha_h) & 3\beta_m & 0 & 0 & \beta_h & 0 \\ 0 & \alpha_m & -(3\beta_m+\alpha_h) & 0 & 0 & 0 & \beta_h \\ 0 & 0 & 0 & -(3\alpha_m+\beta_h) & \beta_m & 0 & 0 \\ \alpha_h & 0 & 0 & 3\alpha_m & -(2\alpha_m+\beta_m+\beta_h) & 2\beta_m & 0 \\ 0 & \alpha_h & 0 & 0 & 2\alpha_m & -(\alpha_m+2\beta_m+\beta_h) & 3\beta_m \\ 0 & 0 & \alpha_h & 0 & 0 & \alpha_m & -(3\beta_m+\beta_h) \end{bmatrix}$$

$S_K$ and $S_{Na}$ are the square root matrices of the following diffusion matrices:

$$D_K = \begin{bmatrix} 4\alpha_n\bar{x}_0+(3\alpha_n+\beta_n)\bar{x}_1+2\beta_n\bar{x}_2 & -3(\alpha_n\bar{x}_1+2\beta_n\bar{x}_2) & 0 & 0 \\ -(3\alpha_n\bar{x}_1+2\beta_n\bar{x}_2) & 3\alpha_n\bar{x}_1+2(\alpha_n+\beta_n)\bar{x}_2+3\beta_n\bar{x}_3 & -(2\alpha_n\bar{x}_2+3\beta_n\bar{x}_3) & 0 \\ 0 & -(2\alpha_n\bar{x}_2+3\beta_n\bar{x}_3) & 2\alpha_n\bar{x}_2+(\alpha_n+3\beta_n)\bar{x}_3+4\beta_n\bar{x}_4 & -(\alpha_n\bar{x}_3+4\beta_n\bar{x}_4) \\ 0 & 0 & -(\alpha_n\bar{x}_3+4\beta_n\bar{x}_4) & \alpha_n\bar{x}_3+4\beta_n\bar{x}_4 \end{bmatrix}$$

$$D_{Na} = \begin{bmatrix} d_1 & -2(\alpha_m\bar{y}_{10}+\beta_m\bar{y}_{20}) & 0 & 0 & -(\alpha_h\bar{y}_{10}+\beta_h\bar{y}_{11}) & 0 & 0 \\ -2(\alpha_m\bar{y}_{10}+\beta_m\bar{y}_{20}) & d_2 & -(\alpha_m\bar{y}_{20}+3\beta_m\bar{y}_{30}) & 0 & 0 & -(\alpha_h\bar{y}_{20}+\beta_h\bar{y}_{21}) & 0 \\ 0 & -(\alpha_m\bar{y}_{20}+3\beta_m\bar{y}_{30}) & d_3 & 0 & 0 & 0 & -(\alpha_h\bar{y}_{30}+\beta_h\bar{y}_{31}) \\ 0 & 0 & 0 & d_4 & -(3\alpha_m\bar{y}_{01}+\beta_m\bar{y}_{11}) & 0 & 0 \\ -(\alpha_h\bar{y}_{10}+\beta_h\bar{y}_{11}) & 0 & 0 & -(3\alpha_m\bar{y}_{01}+\beta_m\bar{y}_{11}) & d_5 & -2(\alpha_m\bar{y}_{11}+\beta_m\bar{y}_{21}) & 0 \\ 0 & -(\alpha_h\bar{y}_{20}+\beta_h\bar{y}_{21}) & 0 & 0 & -2(\alpha_m\bar{y}_{11}+\beta_m\bar{y}_{21}) & d_6 & -(\alpha_m\bar{y}_{21}+3\beta_m\bar{y}_{31}) \\ 0 & 0 & -(\alpha_h\bar{y}_{30}+\beta_h\bar{y}_{31}) & 0 & 0 & -(\alpha_m\bar{y}_{21}+3\beta_m\bar{y}_{31}) & d_7 \end{bmatrix}$$

with diagonal elements:

$$\begin{aligned} d_1 &= 3\alpha_m\bar{y}_{00}+(2\alpha_m+\beta_m+\alpha_h)\bar{y}_{10}+2\beta_m\bar{y}_{20}+\beta_h\bar{y}_{11} \\ d_2 &= 2\alpha_m\bar{y}_{10}+(\alpha_m+2\beta_m+\alpha_h)\bar{y}_{20}+3\beta_m\bar{y}_{30}+\beta_h\bar{y}_{21} \\ d_3 &= \alpha_m\bar{y}_{20}+(3\beta_m+\alpha_h)\bar{y}_{30}+\beta_h\bar{y}_{31} \\ d_4 &= \alpha_h\bar{y}_{00}+(3\alpha_m+\beta_h)\bar{y}_{01}+\beta_m\bar{y}_{11} \\ d_5 &= \alpha_h\bar{y}_{10}+3\alpha_m\bar{y}_{01}+(2\alpha_m+\beta_m+\beta_h)\bar{y}_{11}+2\beta_m\bar{y}_{21} \\ d_6 &= \alpha_h\bar{y}_{20}+2\alpha_m\bar{y}_{11}+(\alpha_m+2\beta_m+\beta_h)\bar{y}_{21}+3\beta_m\bar{y}_{31} \\ d_7 &= \alpha_h\bar{y}_{30}+\alpha_m\bar{y}_{21}+(3\beta_m+\beta_h)\bar{y}_{31} \end{aligned}$$

and where:

$$\bar{x}_i = \binom{4}{i}\frac{\alpha_n^i\beta_n^{4-i}}{(\alpha_n+\beta_n)^4}$$

$$\bar{y}_{ij} = \binom{3}{i}\frac{\alpha_m^i\beta_m^{3-i}\alpha_h^j\beta_h^{1-j}}{(\alpha_m+\beta_m)^3(\alpha_h+\beta_h)}$$

Although these matrices involve a slight approximation to those found in the original Fox and Lu literature [21], simulations showing remarkable agreement between the original Fox and Lu system and the system of equations in Eq. (3) can be found in [22]. The primary purpose of this approximation is to guarantee that the square roots of the diffusion matrices exist.

[1] R. VanRullen, R. Guyonneau, and S. J. Thorpe, Trends in neurosciences **28**, 1 (2005).
[2] W. Gerstner, W. M. Kistler, R. Naud, and L. Paninski, *Neuronal dynamics: From single neurons to networks and models of cognition* (Cambridge University Press, 2014).
[3] F. Rieke, D. Warland, R. De Ruyter van Steveninck, and W. Bialek, "Exploring the neural code," (1999).
[4] S. Thorpe, D. Fize, C. Marlot, *et al.*, nature **381**, 520 (1996).
[5] W. Bialek, F. Rieke, R. d. R. Van Steveninck, and D. Warland, Science **252**, 1854 (1991).
[6] M. Abeles, H. Bergman, E. Margalit, and E. Vaadia, Journal of neurophysiology **70**, 1629 (1993).
[7] M. Abeles, Y. Prut, H. Bergman, and E. Vaadia, in *Temporal coding in the brain* (Springer, 1994) pp. 39–50.
[8] L. M. Optican and B. J. Richmond, Journal of Neurophysiology **57**, 162 (1987).
[9] E. T. Rolls and M. J. Tovee, Journal of Neurophysiology **73**, 713 (1995).
[10] R. S. Petersen, S. Panzeri, and M. E. Diamond, Neuron **32**, 503 (2001).
[11] P. Heil, Current opinion in neurobiology **14**, 461 (2004).
[12] R. S. Johansson and I. Birznieks, Nature neuroscience **7**, 170 (2004).
[13] E. Arabzadeh, S. Panzeri, and M. E. Diamond, The Journal of Neuroscience **26**, 9216 (2006).
[14] Y. Zuo, H. Safaai, G. Notaro, A. Mazzoni, S. Panzeri, and M. E. Diamond, Current Biology **25**, 357 (2015).
[15] M. Von Heimendahl, P. M. Itskov, E. Arabzadeh, and M. E. Diamond, PLoS Biol **5**, e305 (2007).
[16] M. E. Diamond, M. von Heimendahl, P. M. Knutsen, D. Kleinfeld, and E. Ahissar, Nature Reviews Neuroscience **9**, 601 (2008).
[17] A. L. Hodgkin and A. F. Huxley, The Journal of physiology **117**, 500 (1952).
[18] A. Bukoski, D. Steyn-Ross, and M. L. Steyn-Ross, Physical Review E **91**, 032708 (2015).
[19] E. M. Izhikevich, IEEE transactions on neural networks **15**, 1063 (2004).
[20] R. Wells, Moscow, ID: The University of Idaho (2007).
[21] R. F. Fox and Y.-n. Lu, Physical Review E **49**, 3421 (1994).
[22] J. H. Goldwyn, N. S. Imennov, M. Famulare, and E. Shea-Brown, Physical Review E **83**, 041908 (2011).
[23] J. H. Goldwyn and E. Shea-Brown, PLoS Comput Biol **7**, e1002247 (2011).
[24] T. Branco and K. Staras, Nature Reviews Neuroscience **10**, 373 (2009).
[25] C. Allen and C. F. Stevens, Proceedings of the National Academy of Sciences **91**, 10380 (1994).
[26] N. R. Hardingham and A. U. Larkman, The Journal of Physiology **507**, 249 (1998).
[27] N. A. Hessler, A. M. Shirke, and R. Malinow, (1993).
[28] H. Markram and M. Tsodyks, (1996).
[29] H. G. Ferreira and M. W. Marshall, *The biophysical basis of excitability* (Cambridge University Press, 1985).
[30] M. Uzuntarla, M. Ozer, and D. Guo, The European Physical Journal B **85**, 1 (2012).
[31] C. Koch, *Biophysics of computation: information processing in single neurons* (Oxford university press, 2004).
[32] C. Gold, C. C. Girardin, K. A. Martin, and C. Koch, Journal of neurophysiology **102**, 3340 (2009).
[33] A. Torcini, S. Luccioli, and T. Kreuz, Neurocomputing **70**, 1943 (2007).
[34] A. Reyes and B. Sakmann, The Journal of neuroscience **19**, 3827 (1999).
[35] J. Jack, S. Miller, R. Porter, and S. Redman, The Journal of physiology **215**, 353 (1971).
[36] I. Timofeev and M. Steriade, The Journal of physiology **504**, 153 (1997).
[37] A. H. Gittis, S. H. Moghadam, and S. du Lac, Journal of neurophysiology **104**, 1625 (2010).
[38] I. Gold, Consciousness and cognition **8**, 186 (1999).
[39] V. Braitenberg and A. Schüz, *Anatomy of the cortex: statistics and geometry*, Vol. 18 (Springer Science & Business Media, 2013).
[40] C.-C. Lee and J. C. Middlebrooks, Nature neuroscience **14**, 108 (2011).
[41] Y. B. Sirotin, R. Shusterman, and D. Rinberg, eneuro **2**, ENEURO (2015).
[42] D. J. Higham, SIAM review **43**, 525 (2001).
[43] T. C. Gard, *Introduction to stochastic differential equations* (M. Dekker, 1988).
[44] M. Ozer, M. Uzuntarla, M. Perc, and L. J. Graham, Journal of theoretical biology **261**, 83 (2009).
[45] C. P. Billimoria, R. A. DiCaprio, J. T. Birmingham, L. Abbott, and E. Marder, The Journal of neuroscience **26**, 5910 (2006).
[46] S. Luccioli, T. Kreuz, and A. Torcini, Physical Review E **73**, 041902 (2006).
[47] W. J. Wilbur and J. Rinzel, Journal of Theoretical Biology **105**, 345 (1983).
[48] R. G. Steel and H. James, *Principles and procedures of statistics: with special reference to the biological sciences*, Tech. Rep. (New York, US: McGraw-Hill, 1960).
[49] B. L. Benedetti, S. Glazewski, and A. L. Barth, The Journal of neuroscience **29**, 11817 (2009).
[50] A. Saarinen, M.-L. Linne, and O. Yli-Harja, PLoS Comput Biol **4**, e1000004 (2008).
[51] J. M. Casado, Physics Letters A **310**, 400 (2003).
[52] J. Jo, H. Kang, M. Y. Choi, and D.-S. Koh, Biophysical journal **89**, 1534 (2005).
[53] M. Ozer and N. H. Ekmekci, Physics Letters A **338**, 150 (2005).
[54] C. Finke, J. Vollmer, S. Postnova, and H. A. Braun, Mathematical biosciences **214**, 109 (2008).
[55] I. C. Bruce, Annals of biomedical engineering **37**, 824 (2009).
[56] B. Sengupta, S. Laughlin, and J. Niven, Physical Review E **81**, 011918 (2010).
[57] M. Van Rossum, B. J. O'Brien, and R. G. Smith, Journal of neurophysiology **89**, 2406 (2003).
[58] G.-q. Bi and M.-m. Poo, The Journal of Neuroscience **18**, 10464 (1998).
[59] P. J. Uhlhaas and W. Singer, Neuron **52**, 155 (2006).
[60] C. Hammond, H. Bergman, and P. Brown, Trends in Neurosciences **30**, 357 (2007).
[61] K. Abuhassan, D. Coyle, and L. Maguire, Frontiers in Computational Neuroscience **8** (2014).